Journal of Rehabilitation in Civil Engineering 8-2 (2020) 114-125

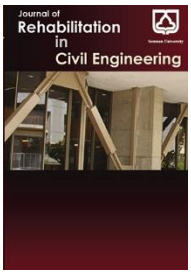

Journal homepage: http://civiljournal.semnan.ac.ir/

Numerical Analysis of Water and Air in Venturi Tube to Produce Micro-Bubbles

M. Ghannadi[1*], S. F. Saghravani[2] and H. Niazmand[3]
1. Ph.D., Faculty member at Islamic Azad University of Sarab Branch, Sarab, Iran
2. Associate Professor, Department of Civil Engineering, Shahrood University of Technology, Shahrood, Iran
3. Professor, Department of Mechanical Engineering, Ferdowsi University of Mashhad, Mashhad, Iran

Corresponding author:*mahin8185saze@yahoo.com*

ARTICLE INFO

Article history:
Received: 10 October 2018
Accepted: 18 December 2019

Keywords:
Two-Phase Flow,
Micro-Bubble,
OpenFOAM,
Venturi Tube,
VOF.

ABSTRACT

Two-phase flow regimes are affected by conduit position, alignment, geometry, flow direction, physical characteristics, and flow rate of each phase as well as the heat flux toward the boundaries. Due to the importance of two-phase flow, numerous regimes have been identified. The first step in studying micro-bubble formation inside a venturi tube is to recognize the type of flow regimes. In this study, which is devoted to the study of micro-bubble formation, a numerical investigation by OpenFOAM software and a VOF model was conducted. Results suggest that flow regime inside the venturi tube is roughly similar to flow regimes inside the horizontal tubes. For having bubble flow and consequently forming micro-bubble, flow rate of gas phase should be very smaller than liquid phase flow rate while the air inlet diameter should be chosen much smaller than water input diameter. Numerical simulations indicate that the best results are achieved for the water velocity of about 1-2m/s.

1. Introduction

When two different phases of fluids (e.g. liquid and gas), having different physical properties, simultaneously flow inside a tube, two-phase flow forms. The interactions between the two phases result in diverse flow patterns that happen randomly [1]. Flow pattern is the distribution of each phase against the other phase, inside the tube in which the fluid flows. The most important sign of two-phase flows is the existence of different interfaces between gas and liquid phases. Theoretically, there is the possibility of emergence of wide range of interfaces among two phases; however, the effect of surface tension between two phases results in the emergence of curved interfaces and then they all transform into spherical shapes (e.g. drops and bubbles) [2].

A large number of petrochemical, chemical, biochemical and other processes use gas

DOI: 10.22075/JRCE.2019.16139.1305

bubbles dispersed in a liquid such as operations in contactors as well as in the reactions namely hydrogenation, polymerization, oxidation, chlorination, alkylation, and fermentation. The use of air bubbles in wastewater treatment is of particular importance [3]. Bubbles ranging from 10 μm to 1000 μm are micro-bubbles, lower than 10 μm are nano-bubbles, and higher than 1000 μm are macro-bubbles [4].

The addition of zeolite and micro-nano bubble water to the mixture have improved the properties of concrete in the chloride conditions [5]. The fine and stable air particles in the water containing micro-nano bubbles accelerate the reaction between the cement and the water. Water containing air micro-nano bubbles, like other nanoparticles, has a positive effect on the mechanical properties of foamed concrete. Water containing air micro-nano bubble increases the compressive strength at 7, 28 and 90 days of age by 18, 13 and 5%, respectively. This water increases flexural strength by 27% and tensile strength by 22%. Reduction of initial and final setting time of concrete by 28 minutes and 30 minutes, reduction of initial and final setting time of foamed concrete foam by 20 minutes and 58 minutes, slight and negligible reduction of water absorption and shrinkage by 1% is other results [6].

Interesting applications of micro-bubbles were found even for their purely mechanical effects like drag reduction in water flows reaching as much as 80% [7]. Moreover, oil-removal washing has also been reported [8]. Another less known application is the therapeutic ultrasound focusing applied in surgery, where the micro-bubbles convert the ultrasonic vibration into a thermal energy [9]. Other advantages that micro-bubbles may offer have received less attention than they deserve since the available methods of micro-bubbles generation tended to be rather expensive and/or inefficient. A promising new solution to this problem was recently found [10,11] in pulsating the supplied gas flow, using fluidic oscillators i.e. simple devices based on hydrodynamic instability and essentially consisting of nothing more than a specially shaped gas inlet [12-14]. While inexpensive and not extracting much energy from the gas flow, the fluidic oscillators are also maintenance-free and robust. Due to the absence of movable and/or deformed mechanical components, they can reach high pulsation frequency and their life span is practically unlimited. When used for micro-bubble production the fluidic, oscillators [15, 16] are mostly positioned in the air inlet into the device called aerator (the term “diffuser”, used by some authors, is not a suitable choice as it has a different standard meaning in general fluid mechanics [17]).

Two-phase flows follow the rules of fluid mechanics; however, in comparison to single-phase flows, there are many factors which contribute to the uncertainty and complexity of two-phase flows. In the other words, two-phase flows are extremely complex, even in the case of one–dimensional two-phase flows inside a pipe. To overcome these complexities, researchers have taken various approaches such as experimenting on simple physical models so that they could be used in the analysis of engineering and scientific problems and finding simpler equations [18].

Generally, one can explain these types of flows by categorizing different states of interfaces between liquid and gas phases, which is so-called regime or flow pattern. It should be noted that flow regimes usually are affected by tube’s position and its geometric

shape, flow direction, physical characteristics, flow rate of each phase, and heat flux entered into the walls of the tube.

Many studies have been done to classify and analyze two-phase flows. For example, Baker et al. have provided a flow map for the two-phase flow inside the tube. The quantities intended for the coordinate axes of this diagram give the possibility of using the diagram for different fluids [19,20]. Mandhane et al have provided a flow chart for liquid-gas with apparent velocities of the phases as coordinate axes [21]. Sandra et al. through FLUENT software, have simulated various flow patterns in Baker's flow diagram; however, they did not obtain favorable results for bubble and slug flow regimes [22]. Krishnan et al. used VOF method and FLUENT commercial code in simulating two-phase flow inside a mini-channel and studied the effect of various numerical methods, and wall adhesion on the quality of the solutions [23]. Ansari et al. have studied the conditions of occurrence of different regimes in the horizontal channel in a two-dimensional fashion and concluded that the VOF method is more suitable for studying different regimes [24,25]. It should also be noted that despite many efforts made for categorizing various two-phase regimes, a great portion of those attempts are based on either the qualitative methods or personal viewpoints of the researchers. So far, many flow regimes have been defined and a very wide range of names have been given to these regimes. Seven types of distribution patterns exist for two-phase flows inside horizontal tubes: bubbly flow, plug flow, stratified flow, wavy flow, slug flow, annular flow, droplet flow [26]. J. X. Zhang [27] have shown that when the contraction ratio is less than 0.2, the velocity has an asymmetric distribution.

The first step in studying micro-bubble formation inside a venturi tube is to recognize the type of flow regimes. In this study, which is devoted to study of micro-bubble formation, a numerical investigation by OpenFOAM software and a VOF model was conducted.

2. Modeling Description and Numerical Solution

Flow in a venturi tube was numerically simulated for a geometry given in Fig. 1. The conduit is composed of the contraction section, the throat section, and the diffusion section. The diameter of the tube is 2.54 cm and the diameter of the throat section is 0.254 cm. A half part of the input was allocated for air inlet and the other half was allocated for water inlet. The length of throat section is 2.54 cm. Mesh dimensions are 0.1 cm.

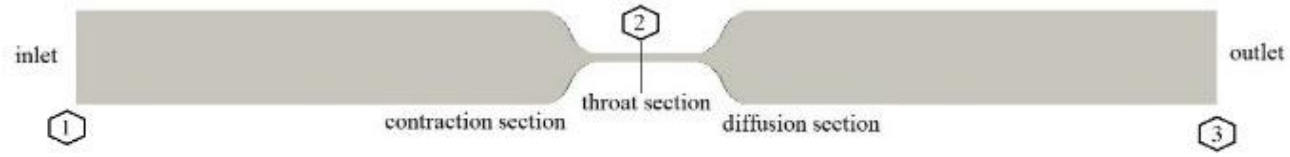

Fig. 1. Schematic of the venturi tube structure.

In this work, the computational facilities of Sheikh Bahaei National High Performance Computing Center (SBNHPCC) were employed for CFD simulation by the use of OpenFOAM. The processor was an AMD Opteron 2.2 GHz, 10 Core and 20 GB RAM. OpenFOAM is an open-source computational fluid dynamic toolbox, written in C++ that is

capable of modeling many types of problems including partial differential equations. OpenFOAM is also capable of solving a range of simple to complex numerical fluid flow problems. OpenFOAM has solvers which can be developed and edited further. It employs finite-volume method (FVM) in solving partial differential equations. Gambit software was used in constructing geometry and meshing the model. ParaView software was used to generate graphical results. InterFOAM solver was used for solving which is embedded in OpenFOAM software. This solver is used in modeling two-phase fluid flow and it is based on the shared surface control. The ratio of the phases is determined by volume-of-fluid method (VOF). In the volume-of-fluid method, solving the flow is done by momentum equation and continuity equation [28,29].

The Reynolds-averaged Navier–Stokes equations (RANS) in cartesian coordinate system are as follows [30]:

Continuity equation:

$$\frac{\partial \rho}{\partial t} + \frac{\partial (\rho u_i)}{\partial x_i} = 0 \quad (1)$$

Momentum equation:

$$\frac{\partial (\rho u_i)}{\partial \mathrm{t}} + \rho \frac{\partial}{\partial x_j}(u_i u_j) = -\frac{\partial P}{\partial x_i} + \frac{\partial}{\partial x_j}\left[\mu\left(\frac{\partial u_i}{\partial x_j} - \rho\overline{\acute{u}_\iota \acute{u}_j}\right)\right] \quad (2)$$

where, u_i is the average velocity towards *i*, ρ is water density, *P* is the static pressure, μ is the viscosity, $-\rho\overline{\acute{u}_\iota \acute{u}_j}$ is the Reynolds stress, and i,j=1,2,3(x,y,z).

The relationship between Reynolds stress and changes in average velocity is given by Boussinesq hypothesis:

$$-\rho\overline{\acute{u}_\iota \acute{u}_j} = \mu_t\left(\frac{\partial \overline{u}_\iota}{\partial x_j} + \frac{\partial \overline{u}_j}{\partial x_i}\right) - \frac{2}{3}\delta_{ij}\rho k \quad (3)$$

where μ_t and k are turbulent viscosity (eddy viscosity) and turbulent kinetic energy, respectively.

Equations for turbulent kinetic energy (κ) and dissipation rate of turbulent kinetic energy (ε) in standard κ-ε model are as follows:

Turbulent kinetic energy equation:

$$\frac{\partial}{\partial t}(\rho k) + \frac{\partial}{\partial X_i}(\rho k U_i) = \frac{\partial}{\partial X_j}\left[\left(\mu + \frac{\mu_t}{\sigma_k}\right)\frac{\partial k}{\partial X_i}\right] + G_k + G_b - \rho\varepsilon - Y_M \quad (4)$$

Dissipation equation:

$$\frac{\partial}{\partial t}(\rho \varepsilon) + \frac{\partial}{\partial X_i}(\rho \varepsilon U_i) = \frac{\partial}{\partial X_j}\left[\left(\mu + \frac{\mu_t}{\sigma_\varepsilon}\right)\frac{\partial \varepsilon}{\partial X_i}\right] + C_{1\varepsilon}\frac{\varepsilon}{k}(G_k + C_{3\varepsilon}G_b) + C_{2\varepsilon}\rho\frac{\varepsilon^2}{k} \quad (5)$$

where,

$\mu_t = \rho C_\mu \frac{k^2}{\varepsilon}$.

In the equations above G_k and G_b are the production rate of turbulent kinetic energy due to floating and velocity changes, Y_M is dilatation dissipation, $C_{1\varepsilon}$,$C_{2\varepsilon}$,$C_{3\varepsilon}$, and C_μ are fixed values, σ_k and σ_ε are turbulent Prandtl numbers for *K* and ε ,respectively.

OpenFOAM software uses finite-volume Method in solving equations. Volume-of-

Fluid method is used for the purpose of modeling. VOF was proposed by Hirt. [30]. The method is based on the idea of a so-called fraction function α. It is a scalar function, defined as the integral of a fluid's characteristic function in the control volume, namely, the volume of a computational grid cell. The volume fraction of each fluid is tracked through every cell in the computational grid, while all fluids share a single set of momentum equations. When a cell is empty with no traced fluid inside, the value of α is zero; when the cell is full, α = 1; and when there is a fluid interface in the cell, 0 < α < 1.

The evolution of the q^{th} fluid in a system on *n* fluids is governed by the transport equation:

$$\frac{\partial \alpha_q}{\partial_t} + \nabla \cdot \left(U \cdot \alpha_q\right) = 0 \quad (6)$$

where, α_q is the volume fraction of fluid of q^{th} phase. Since the purpose of this research is to study micro-bubble formation in a Venturi tube and alpha, the scalable models cannot be used [31]. In this paper, in order to study flow regimes in venturi tube, simulations of liquid and gas flow were made by various velocities based on Table 1.

Table 1. Velocity of air and water phase in venture tube.

Models	Vair (m/s)	Vwater (m/s)
Mode 1	0.05	0.5
Model 2	0.05	1
Model 3	0.05	2
Model 4	0.05	5
Model 5	0.05	10
Model 6	0.1	0.5
Model 7	0.1	1
Model 8	0.1	2
Model 9	0.1	5
Model 10	0.1	10

3. Results and Discussion

In this research, researchers examined flow regimes inside venturi tube concerning micro-bubble formation, using VOF method. Fig. 2 shows the distribution of alpha along the venturi tube and flow regimes for models 1-10. Results show that the wavy flow appears while the velocity of water is 0.5m/s and the velocity of air is less than 0.1 m/s, and the stratified flow appears while the velocity of water is 1 m/s and the velocity of air is 0.1 m/s.

When the velocity of water is more than 2 m/s and the velocity of air is less than 0.1 m/s, the bubbly flow appears and the micro-

bubbles may be produced. In this study, the mesh dimensions are 0.1 cm. In the future studies, smaller meshes will be used to investigate the formation of micro-bubbles.

Fig. 3 shows the distribution of velocity along the venturi tube for models 1-10. Based on the results, the velocity shows an asymmetric distribution in the venturi tube. In this research the contraction ratio is 0.1, The obtained results confirm the results of Zhang's statements. He has showed that when the contraction ratio is less than 0.2, the velocity has an asymmetric distribution. Based on these results, for saving the time of solving and the memory of computer, we cannot use the symmetry for boundary conditions in future studies.

Fig. 4 shows the flow vectors along the venturi tube for models 1-10. As shown in Fig. 4, vortices are formed. Due to the formation of vortices, the bubbles at this place rotate around themselves and cannot get out of the venturi tube and then are confined. In future studies, we will try to reduce this by changing the dimensions of the Venturi tube.

Fig. 5 shows the distribution of pressure along the venturi tube for models 1-10. This figure shows that the pressure distribution is asymmetric.

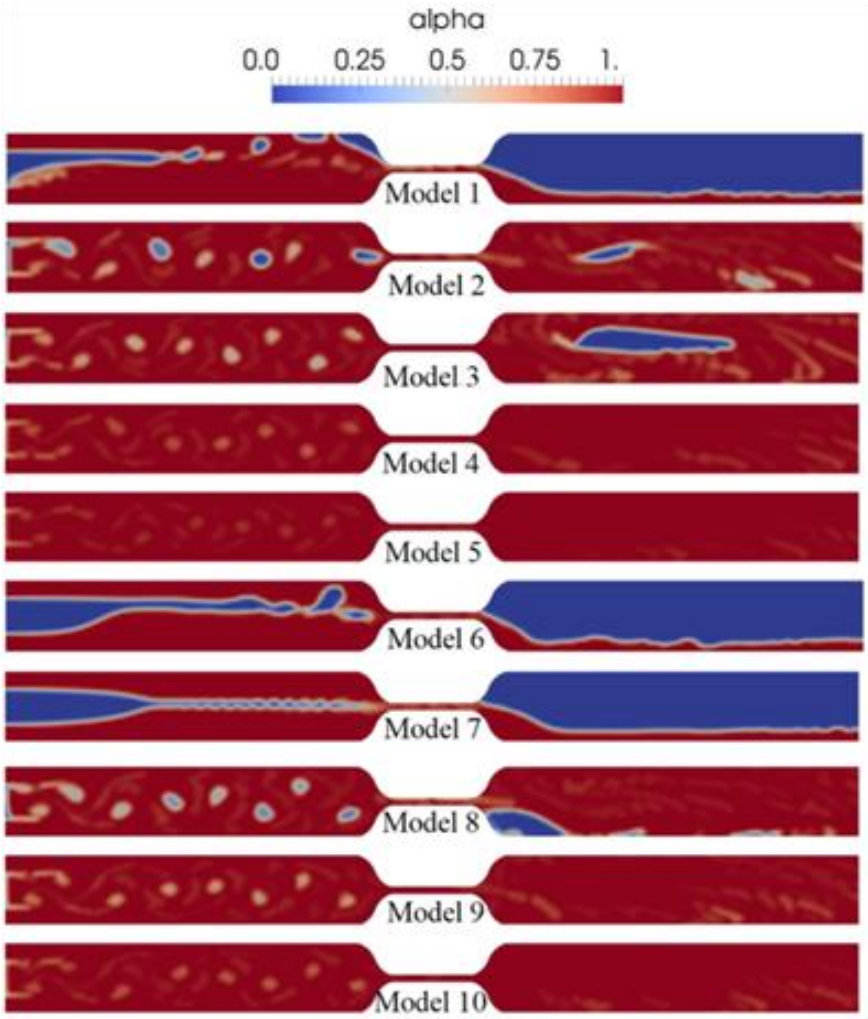

Fig. 2. Alpha distribution for models 1-10, 1 means water and 0 means air.

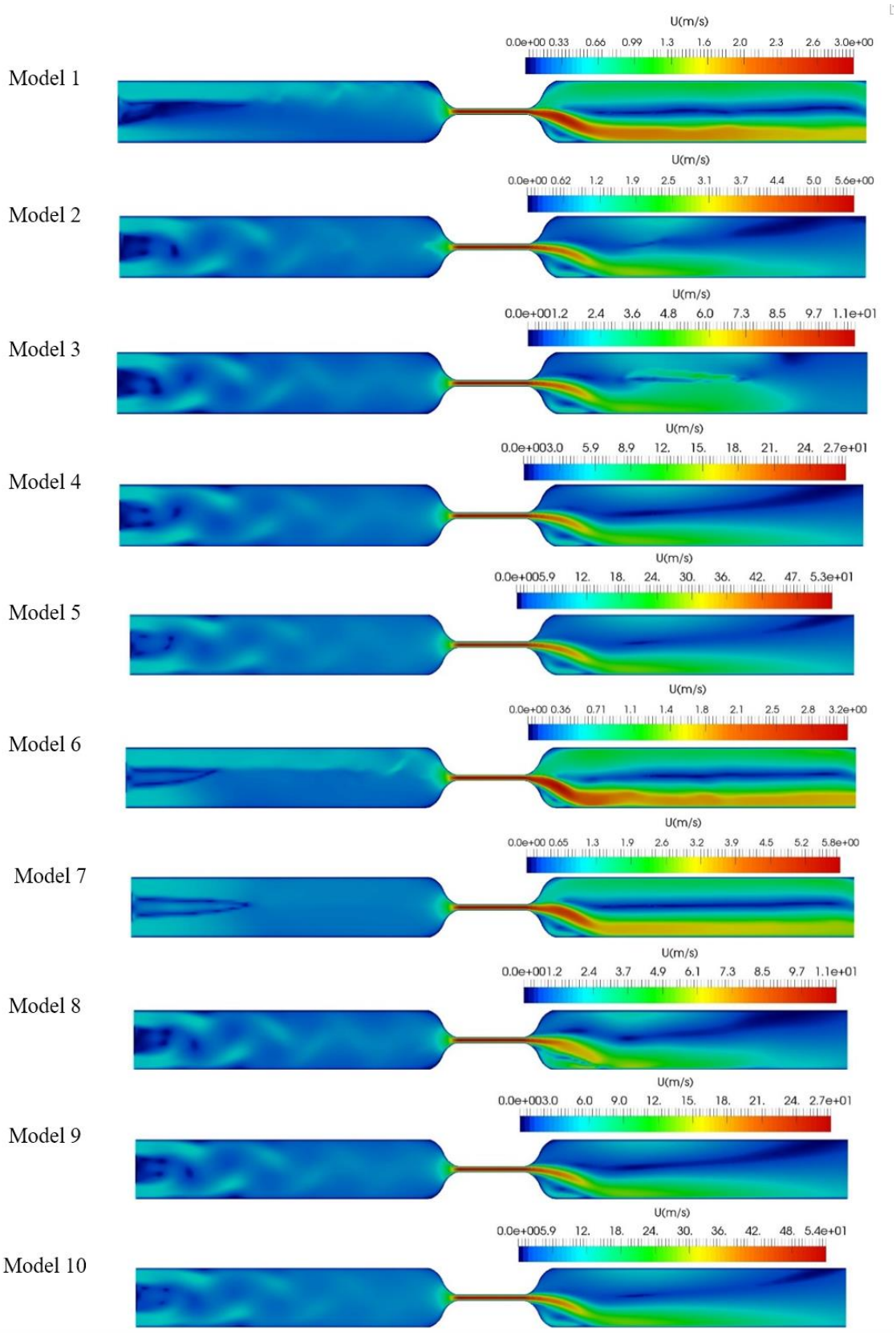

Fig. 3. Velocity distribution for models 1-10

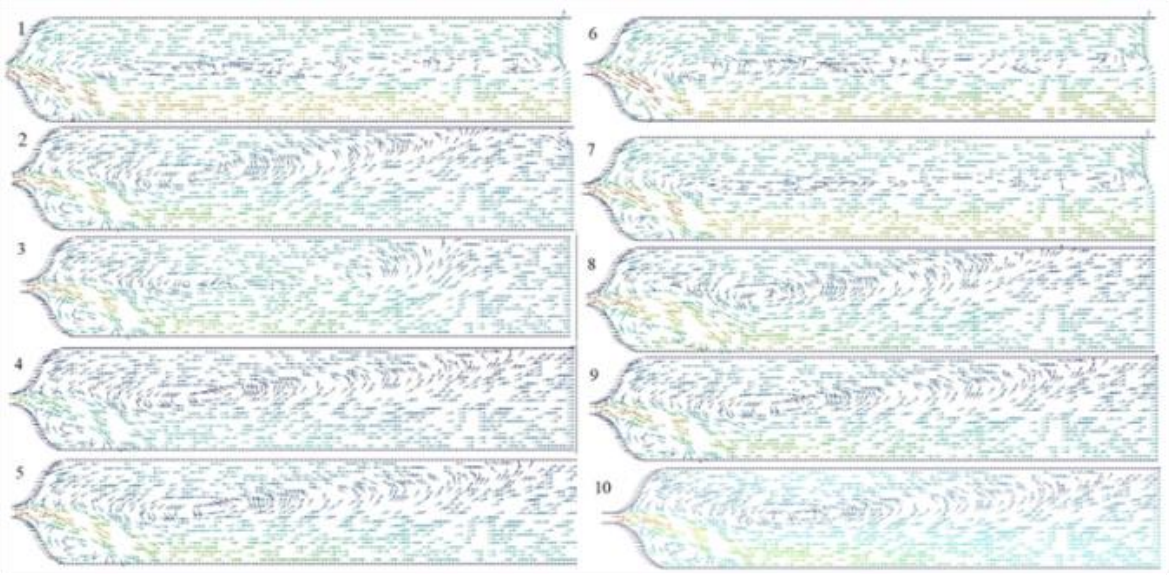

Fig. 4. Flow Vectors for models 1-10.

Table 2. Pressure difference in venture tube.

Models	Vair (m/s)	Vwater (m/s)	p1 (Pa)	p2 (Pa)	p3 (Pa)	Δp1=p1-p2	Δp2=p1-p3	Δp3=p3-p2
Mode1 1	0.05	0.5	3151.05	-847.582	0	3998.632	3151.05	847.582
Model 2	0.05	1	11454.5	-5111.06	0	16565.56	11454.5	5111.06
Model 3	0.05	2	44019.9	-20722.3	0	64742.2	44019.9	20722.3
Model 4	0.05	5	263993	-122473	0	386466	263993	122473
Model 5	0.05	10	1019610	-488455	0	1508065	1019610	488455
Model 6	0.1	0.5	4646.6	-1190.97	0	5837.57	4646.6	1190.97
Model 7	0.1	1	13510.5	-4294.15	0	17804.65	13510.5	4294.15
Model 8	0.1	2	45342.7	-20589.2	0	65931.9	45342.7	20589.2
Model 9	0.1	5	270252	-123505	0	393757	270252	123505
Model 10	0.1	10	1032760	-494102	0	1526862	1032760	494102

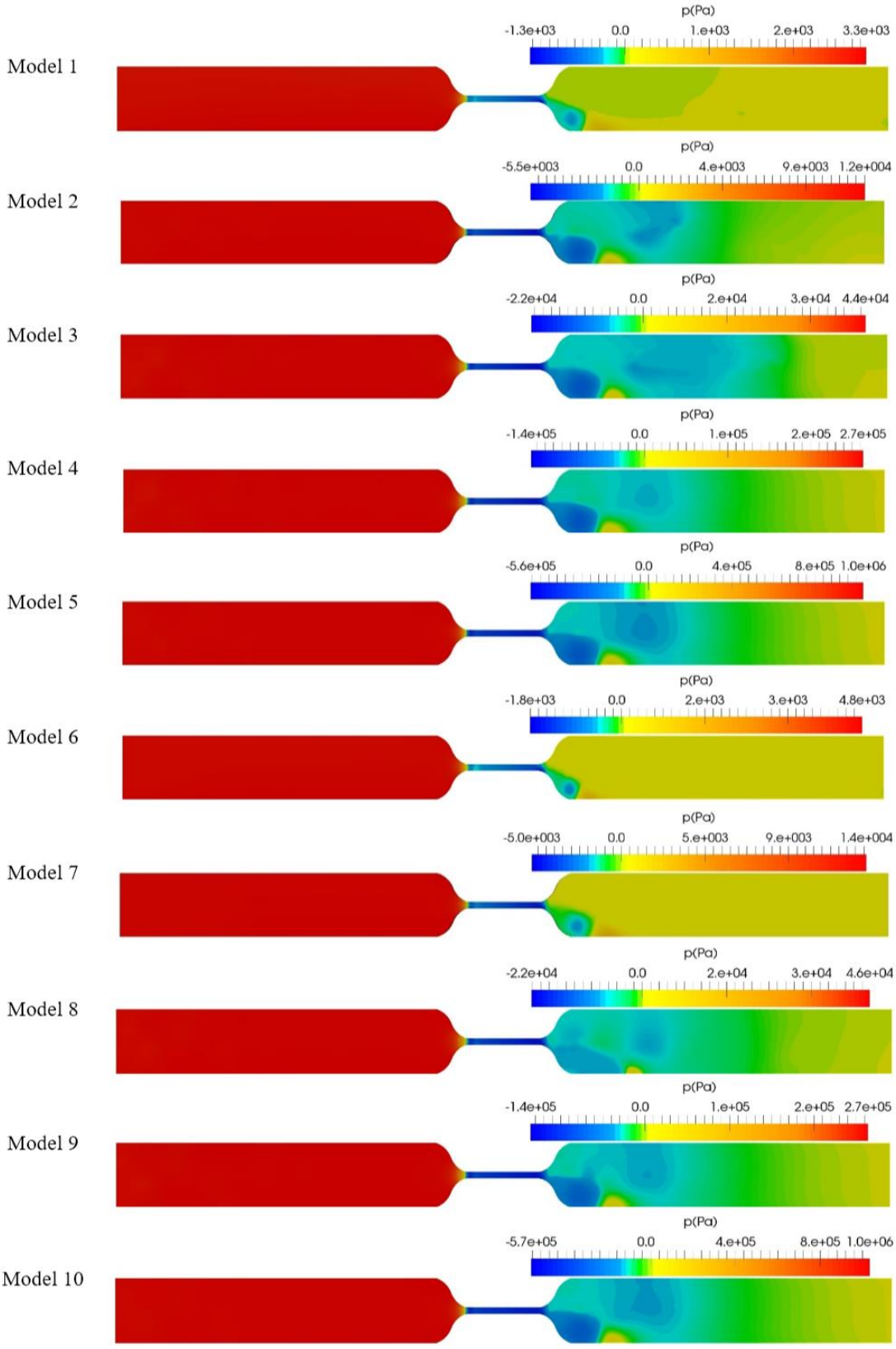

Fig. 5. Pressure distribution for models 1-10

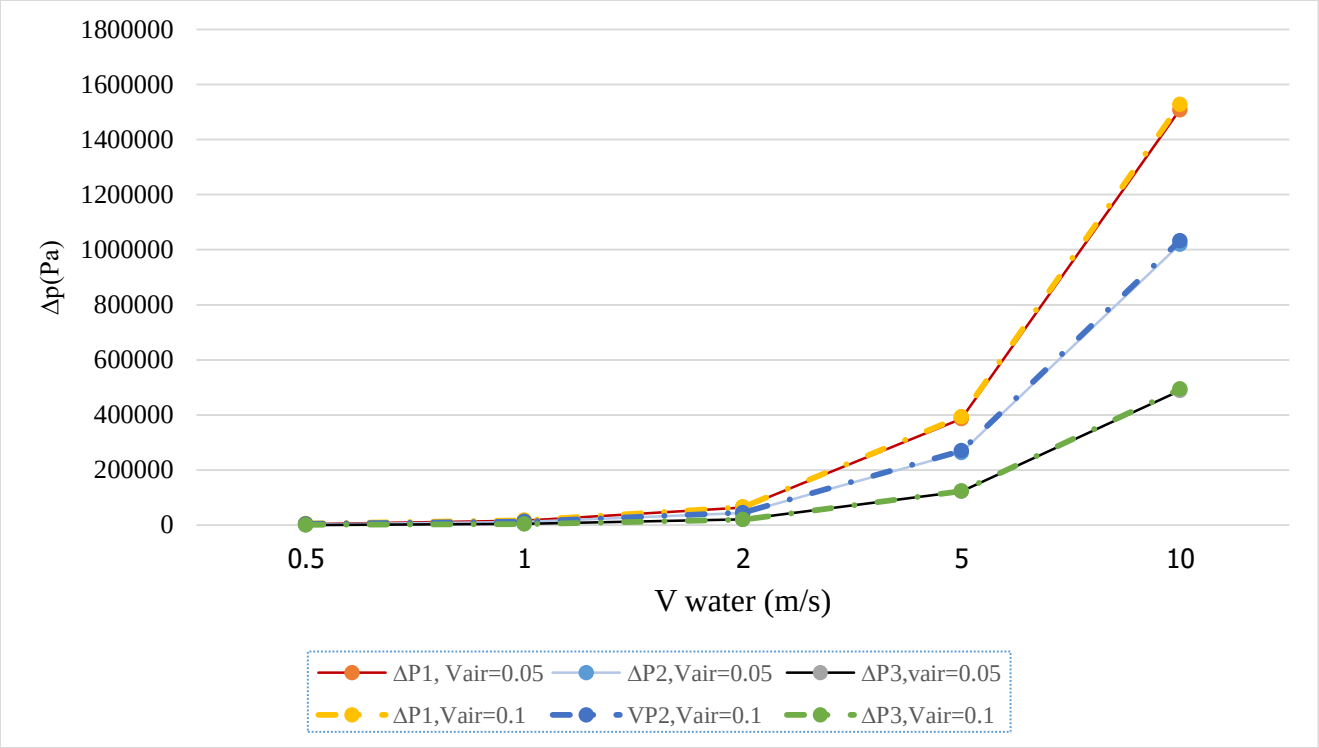

Fig. 6. Δp1=p1-p2, Δp2=p1-p3 and Δp3=p3-p2 for different values of velocity..

Table 2 and Fig. 6 show pressure difference between sections 1 and 2 (Δp1=p1-p2), 1 and 3 (Δp2=p1-p3) and between sections 2 and 3 (Δp3=p3-p2). Results show that when the water velocity is less than 2 m/s, the pressure loss occurs with a low slope. Therefore, in order to have a bubbly flow with less pressure drop, it is better for the velocity of water to be less than 2 m/s.

4. Conclusions

In this research, flow regimes inside venturi tube concerning micro-bubble formation, using VOF method with the OpenFOAM software were considered. So, for Micro-bubble formation inside venturi tube and having bubbly flow:

1- The gas velocity must be smaller than water velocity.

2- To conserve the energy of flow, it is better for the velocity of water to be less than 2m/s and for having a bubbly flow regime, it is better for the velocity of water to be more than 1m/s, and it is better that the velocity of water to be about 1-2m/s.

3- Since the contraction ratio is less than 0.2 (in presented models is 0.1), the velocity, pressure, and alpha distributions are asymmetric, so we cannot use symmetry condition in these studies.

4- The results also show that in order to achieve desired results in producing micro-bubble, the air inlet section relative to the water inlet section must be very small to form a smaller initial bubble. Then, these small bubbles, passing through venturi tube, become broken and finer.

REFERENCES

[1] Martin, CS.,' (1976),Entrapped air in pipelines', Proceeding of the second international conference on pressure

purges, London, September 22-24, , BHRA Fluid Enginnering,Cranfiled, Bedford,England.

[2] Hewitt,G., and Taylor,N.S., (1970),Annular two-phase flow, Pergamon Press, Oxford.

[3] Zimmerman W. B. et al., Evaporation dynamics of Micro-bubbles, Chemical Engineering Science, Vol. 101, p. 865, 2013.

[4] Prevenslik T.: "Stability of nanobubbles by quantum mechanics", Proc. of Conf. 'Topical Problems of Fluid Mechnics',p. 113, Prague 2014.

[5] katebi, A., khoshroo, M., shirzadi javid, A. (2017). 'The evaluation of concrete properties containing zeolite and micro-nano bubble water in the chloride curing condition', Amirkabir Journal of Civil Engineering, doi: 10.22060/ceej.2017.13603.5446.

[6] Soltani H., (2017), The effect of Nano bubbles on cellular lightweight concrete, MSc. Thesis, Shahrood university of technology, Shahrood, Iran.

[7] Madavan N.K. et al., Reduction of turbulent skin friction by Micro-bubbles, Physics of Fluids, Vol.27, p.356, 1984.

[8] Wataneabe K., et al.: Washing effect of Micro-bubbles, Paper OS1-01-1, Proc. of FLUCOME 2013, 12th Intern. Conf., Nara, Japan, November 2013.

[9] Kanagawa T.: Focused ultrasound propagation in water containing many therapeutical Micro-bubbles, Paper OS6-04-4, Proc. of FLUCOME 2013, 12th Intern. Conf., Nara, Japan, November 2013.

[10] Zimmerman W.B., Tesař V.: Bubble generation for aeration and other purposes, British Patent GB20060021561, Filed Oct. 2006.

[11 Zimmerman W. B. et al., Micro-bubble generation, Recent Patents in Engineering, Vol. 2: p.1, 2008.

[12] Raghu S.: Fluidic oscillators for flow control, Experiments in Fluids, Vol. 54, p. 1455, 2013.

[13] Gregory J. W., Tomac M. N.: A review of fluidic oscillator development and application for flow control, 43rd Fluid Dynamics Conf., Code 99250, 201.

[14] Tesař V.: Configurations of fluidic actuators for generating hybrid-synthetic jet Sensors and Actuators A: Physical, Vol. 138, p. 394, 2007.

[15] Tesař V., Zhong S., Fayaz R.: New fluidic oscillator concept for flow separation control, AIAA Journal, Vol. 51, p. 397, 2013.

[16] Tesař V., Hung C.-H., Zimmerman W. B. J.: No-moving-part hybrid-synthetic jet actuator, Sensors and Actuators, A: Physical, Vol. 125, p. 159, 2006.

[17] Kline,S. J., J. P. (1986). Diffusers - flow phenomena and design. In Advanced Topics in Turbomachinery Technology. Principal Lecture Series, No. 2. (D. Japikse, ed.) pp. 6-1 to 6-44, Concepts, ETI, 1986

[18] Mattew,P. and Peramaki,P.E., and Mark,D., And Nelson,P.E.,(2000), 'The significance of two-phase flow regimes in designing multi-phase extractin systems, LBG Article, www.lbgweb.com.

[19] Baker, O.,(1954) 'Simultaneous flow of oil and gas', Oil Gas J., 53, 185–195.

[20] Baker,O., (1975), 'Gas=liquid flow in pipeline, II.Design manual', AGA-API project NX-28,.

[21] Mandhane J.M., Gregory G.A., Aziz K., (1974), 'A flow pattern map for gas–liquid flow in horizontal pipes', Int. J. Multiphase Flow, vol. 1, pp 537–553.

[22] Sandra C.K. De Schepper, Heynderickx G.J., Marin G.B., (2008), 'CFD modeling of all gas–liquid and vapor–liquid flow regimes predicted by the Baker chart', Chemical Engineering journal, vol. 138, pp 349–357.

[23] Krishnan R. N. , Vivek S. , Chatterjee D. , Das S. K.,(2010), 'Performance of numerical schemes in the simulation of two-phase free flows and wall bounded mini channel flows', Chemical

Engineering Science journal, vol. 65 , pp 5117–5136.

[24] Ansari M.R.,)1989(, 'Slug mechanism in horizontal duct and simulation based on one-dimensional two-fluid dynamics', Ph.D. Thesis,Tsukuba University, Japan.

[25] Ansari M.R., Daramizadeh A.,)2012(, 'Slug type hydrodynamic instability analysis using a five equations hyperbolic two-pressure, two-fluid model', Ocean Engineering journal, vol. 52 , pp 1–12.

[26] Levy,S., (1999), 'Two-phase flow in complex systems', John Wiley & Sons, Inc., New York,.

[27] J. X. Zhang, Analysis on the effect of venturi tube structural parameters on fluid flow, AIP ADVANCES 7, 065315 (2017).

[28] H.Nilsson, H.jasak. source forge. OpenFOAM extension.[online], http//www.sourceforge.net.

[29] David C. Wilcox Turbulence modeling for CFD, third edition, DCW industries, Inc. 2006.

[30] C. W. HIRT AND B. D. NICHOLS, Volume of Fluid (VOF) Method for the Dynamics of Free Boundaries, JOURNAL OF COMPUTATIONAL PHYSICS 39, 201-225 (1981)

[31] M.Ghannadi, S.F. Saghravani, H.niazmand, Dimensional analysis in the Study of Micro-Bubble Production Inside Venturi Tube, Trans. Phenom. Nano Micro Scales, 7(1), Winter and Spring 2019, DOI: 10.22111/tpnms.2018.23378.1139.